# Spectrometrically monitored selection experiments: quantitative laser desorption mass spectrometry of small chemical libraries

Kurt Berlin, Rishi K Jain, Charles Tetzlaff, Christoph Steinbeck and Clemens Richert

**Background:** Selection experiments involving chemical libraries are routinely used in the pharmaceutical industry for finding and optimizing lead compounds. In principle, almost any process involving a binding event or a reaction could be probed systematically with chemical libraries prepared by combinatorial synthesis. Traditionally, however, the vast majority of library members cannot be monitored during the selection, making a systematic correlation of structure and activity difficult. To interpret selection experiments on the level of all library components, monitoring technologies are required that give a unique and quantitative spectroscopic signal for every compound in a mixture.

**Results:** Quantitative matrix-assisted laser desorption mass spectrometry of libraries of porphyrins and peptide–DNA hybrids consisting of 2–35 compounds is described. Porphyrin libraries were subjected to *in vitro* selections for liposome incorporation and binding to a protein pocket. It was shown that meso-hydroxyphenyl substituted porphyrins, known high activity photosensitizers of tumors, are preferentially incorporated in liposome membranes. A mixture of peptide–DNA hybrids was assayed for the nuclease stability of its components.

**Conclusions:** Small libraries of non-isobaric compounds can be exhaustively or near-exhaustively monitored by mass spectrometry. Monitored selection experiments can yield detailed structure–activity maps in a single experiment, speeding up drug discovery and the probing of biochemically relevant recognition events. It is proposed that monitored assays for target binding, membrane partitioning, and biostability could be run in parallel, to select drug candidates combining several favorable properties in 'multidimensional' selection experiments.

Address: Department of Chemistry, Tufts University, 62 Talbot Avenue, Medford, MA 02155, USA.

Correspondence: Clemens Richert
E-mail: CRichert@Emerald.Tufts.Edu

**Key words:** combinatorial chemistry, *in vitro* selection, matrix-assisted laser desorption mass spectrometry, peptide–DNA hybrids, porphyrins

Received: **21 November 1996**
Revisions requested: **12 December 1996**
Revisions received: **24 December 1996**
Accepted: **2 January 1997**

Electronic identifier: **1074-5521-004-00063**

**Chemistry & Biology** January 1997, 4:63–77



## Introduction

Combinatorial synthesis allows for the efficient preparation of large collections of related compound with diverse chemical properties (libraries) [1]. Such libraries should be ideal tools for systematically probing molecular interactions, particularly when these interactions can be assayed in *in vitro* selection experiments. So far, however, most studies employing combinatorial synthesis and *in vitro* selection have not been aimed at establishing broad structure–activity relationships [2] or detailed maps of structure space related to chemical properties such as reactivity [3]. This might be due in part to technological limitations. Traditionally, quantitatively tracking the fate of all compounds contained in a library undergoing *in vitro* selection requires extensive separation and many analyses. In principle, libraries of limited size could be exhaustively monitored by spectroscopic techniques, provided that every component gives rise to a selectively detectable spectroscopic signal. Techniques such as NMR-, IR-, UV-, and fluorescence-spectroscopy do not produce a single, resolved, and accurately predictable peak for every component of a library. It is often difficult to analyze mixtures of two compounds because of severe peak overlap. Electrospray ionization (ESI) [4] and matrix-assisted laser desorption (MALDI-TOF) [5,6] mass spectrometry (MS), however, produce essentially fragmentation-free spectra with a pseudomolecular ion peak for every component. For ESI, spectra are usually calculated from spectra containing peaks of several charged states of the analytes. Both ESI and MALDI-TOF MS have been employed for the analysis of mixtures [7]. Laser desorption MS tolerates the presence of buffer salts, impurities and enzymes, and analytes have been detected in crude cell lysates [8]. Thus, MALDI-TOF is particularly suited for work with libraries prepared in combinatorial syntheses, provided that the molecular weights of the individual compounds are non-identical and that their individual mass peaks are distinguishable.

Recently, several studies focused on using mass spectrometry for analyzing selection assays have been reported. It has been demonstrated that ESI Fourier transform ion cyclotron resonance mass spectrometry combined with collision-induced dissociation can be used to simultaneously

screen the inhibitory efficiency of compounds contained in benzene sulfonamide libraries with a randomized dipeptide unit [9,10]. All inhibitors that were sufficiently tightly bound to an enzyme were detected simultaneously, albeit without distinguishing between isomers (a limitation inherent to mass spectrometry). Neutral loss mass spectrometry of heptapeptide libraries featuring one variable residue was used to study the substrate specificity of an antibiotic-synthesizing enzyme [11]. Peptide ladders (mixtures of sequence-related peptides) have been employed for mapping protein–protein interactions by 'affinity-directed' MALDI-TOF MS [12]. Ladders resulting from proteolytic degradation were analyzed to study protein–protein [13], and protein–DNA [14] interactions. A comparison between calculated and measured fast atom bombardment mass spectra of tetrapeptide libraries has also been reported [15], albeit without quantitative analysis of the heavily overlapping peaks.

The studies outlined above focused on peptide libraries and libraries of amino-acid-substituted benzene sulfonamides. Peptides are a class of compounds whose combinatorial synthesis and ESI and MALDI-TOF MS are well established. The physicochemical properties of most small molecule drugs and model compounds typically employed in bioorganic and physical organic chemistry are different, however. Since MALDI-TOF MS is usually associated with poor shot-to-shot reproducibility, it was unclear whether chemically diverse non-peptoid analytes could be monitored accurately with this technique, and if so, what molecular weight differences would be required for detection of individual components. Here, we report that selection experiments involving small combinatorial libraries of porphyrins can be monitored by quantitative MALDI-TOF MS, resulting in a detailed structure–activity map for these comparatively small, heterocyclic compounds. Porphyrins have

**Figure 1**

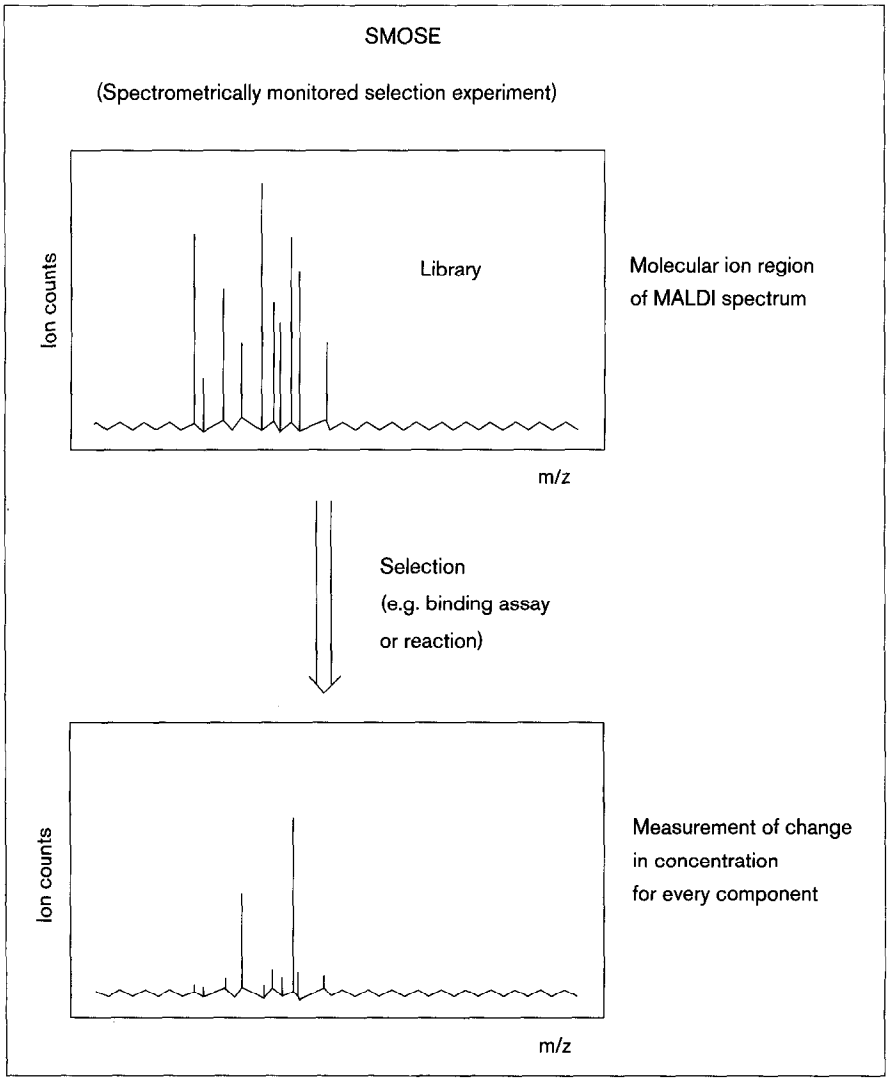


Schematic representation of the analyses underlying mass spectrometrically monitored selection experiments. A library whose components can be quantitatively detected in a single MALDI-TOF mass spectrum is subjected to a selection assay. The change in the concentration of every component can be measured simultaneously. These changes in concentration may be induced by selection conditions involving the binding to a target, partitioning into a new phase, or a chemical reaction.

attracted interest [16] as sensitizers for photodynamic therapy of tumors [17,18]. Porphyrin mixtures were subjected to two different *in vitro* selection experiments to determine structure–activity relationships: a low specificity membrane incorporation assay and a more specific protein–cofactor binding assay. We refer to these assays as spectrometrically monitored selection experiments or 'SMOSEs' (Fig. 1). We have extended the SMOSE methodology to peptide–DNA hybrids, highly charged fragile hybrids of natural biomolecules, and potential inhibitors of gene expression with tunable targeting properties [19–21]. A nuclease assay for selecting biostable hybrids was established.

## Results

There are three ways in which our results may be considered advancements in MALDI-TOF monitoring technology. First, we have found experimental conditions that lead to a simultaneous, efficient desorption of a large number of chemically diverse non-peptoid compounds. Second, we have adjusted these conditions such that the concentration of individual compounds can be measured over an appreciable concentration range. And third, we have established selection assays that are compatible with quantitative MALDI-TOF monitoring. The three different classes of compounds employed in this work are displayed in Figure 2.

**Figure 2**

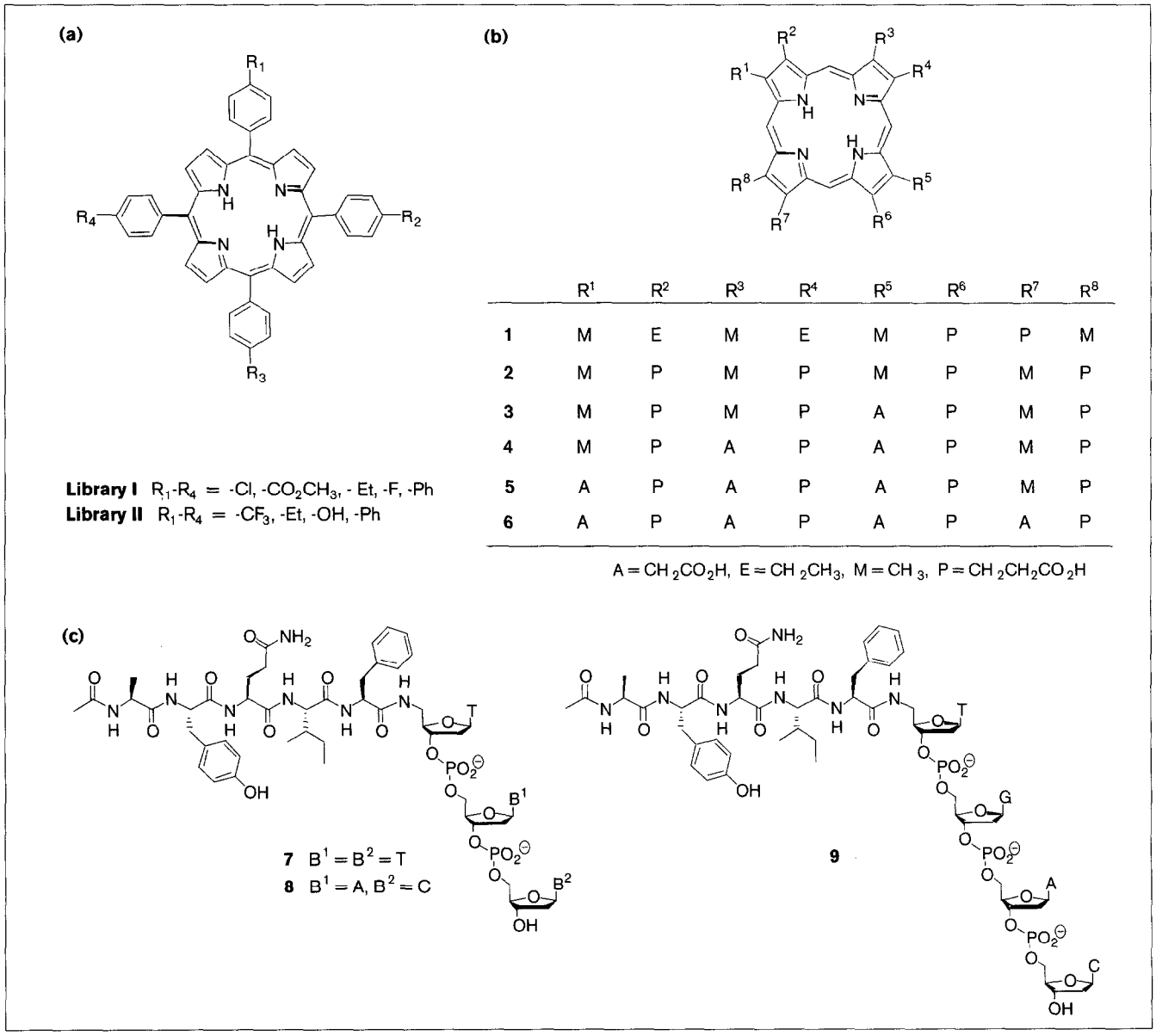


| | R1 | R2 | R3 | R4 | R5 | R6 | R7 | R8 |
|---|---|---|---|---|---|---|---|---|
| 1 | M | E | M | E | M | P | P | M |
| 2 | M | P | M | P | M | P | M | P |
| 3 | M | P | M | P | A | P | M | P |
| 4 | M | P | A | P | A | P | M | P |
| 5 | A | P | A | P | A | P | M | P |
| 6 | A | P | A | P | A | P | A | P |

Structural formulae of **(a)** tetraphenylporphyrin libraries, **(b)** porphyrin acids and **(c)** peptide–DNA hybrids employed in this work.

### Choice of libraries

Libraries to be used in SMOSE experiments should be chosen so that they contain a small number of, or preferably no, isobaric compounds, while still showing the required diversity in their recognition properties. Starting from a given invariable backbone or molecular scaffold, and a specific combinatorial synthetic chemistry scheme, the number of combinatorial steps in the synthesis of a library and the number and identity of building blocks used in this step has to be decided upon. This process was critical for our work with moderately complex tetraphenylporphyrin libraries. We used the computer program MASP [22] (MASP will be available on the world wide web under the GNU public license at http://www.tufts.edu/~csteinbe/MASP) for selecting building blocks for library synthesis. MASP predicts isotopically resolved mass spectra of chemical libraries. MASP can also be used to screen meta-library structure space of potential libraries to be prepared from different combinations of a set of building blocks, and it ranks all possible libraries according to the degree of peak overlap in their mass spectra. A search of meta-library structure space involving the porphyrin core and selected para-substituted meso-phenyl substituents (Br, $CF_3$, Cl, CN, $CO_2Me$, Et, F, H, OH, and Ph) showed that libraries made from five different building blocks gave mass spectra with significantly overlapping peaks for every library generated. This is shown in Figure 3a for **Library I** containing 70 non isomerically-related compounds. Peak heights reflect the number of isobaric components in the library, some of which are identical due to the $D_{4h}$ symmetry of the porphyrin scaffold. The chemical composition of this library is shown in Figure 2a. 38 compounds in the library cannot be unambiguously quantified in this spectrum due to peak overlap. Subsequently, libraries to

**Figure 3**

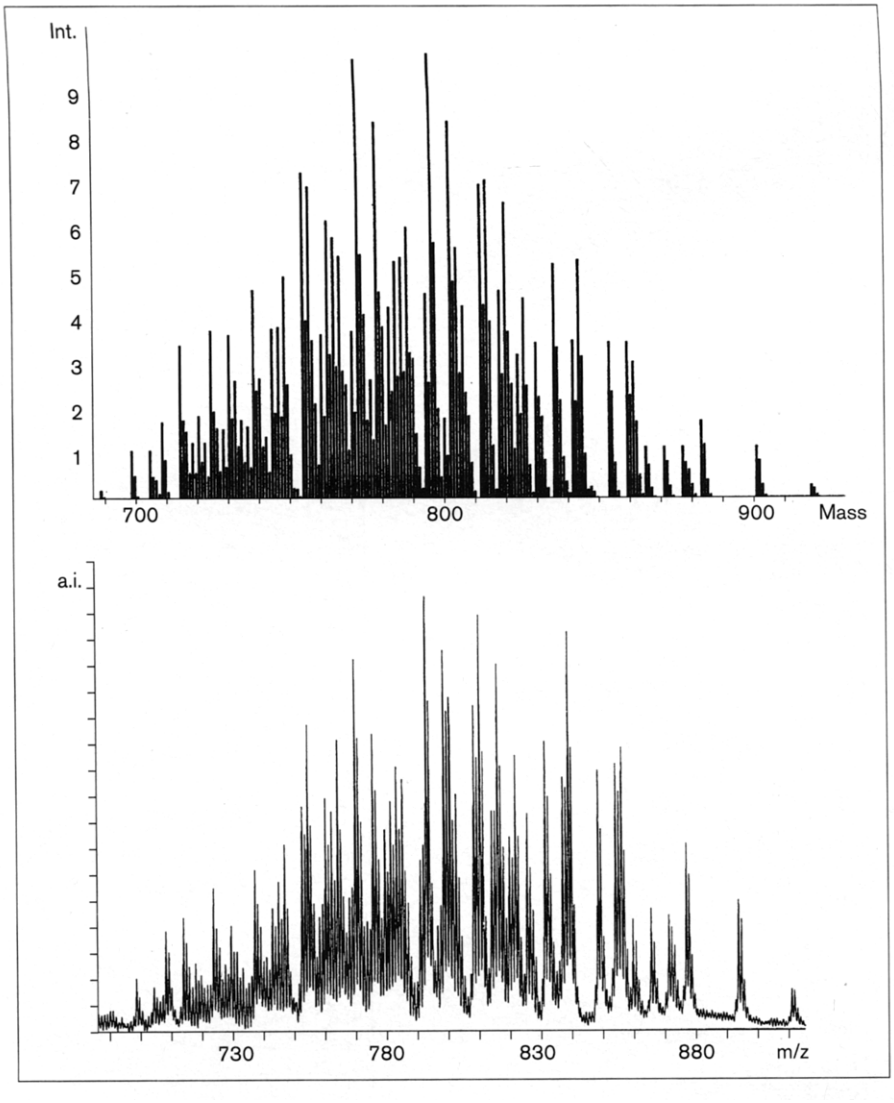


Mass spectrum of **Library I**. Top spectrum, predicted isotopically-resolved mass spectrum of **Library I** generated with the computer program MASP and bottom spectrum, experimental MALDI-TOF mass spectrum of **Library I**. This library contains 70 non-isobaric compounds, each of which is producing a set of isotope peaks. Peak intensity deviations from the predicted spectrum (top) are due to different reactivities of building blocks used in the combinatorial synthesis.

**Figure 4**

Typical quantitative MALDI-TOF mass spectrum of **Library II** at different concentrations using tetraphenylporphyrin (TPP) as internal standard. Top spectrum 10× and middle spectrum 3× the concentration of the bottom spectrum (36, 10.8, and 3.6 pmoles porphyrins total). See the Materials and methods section for experimental details.

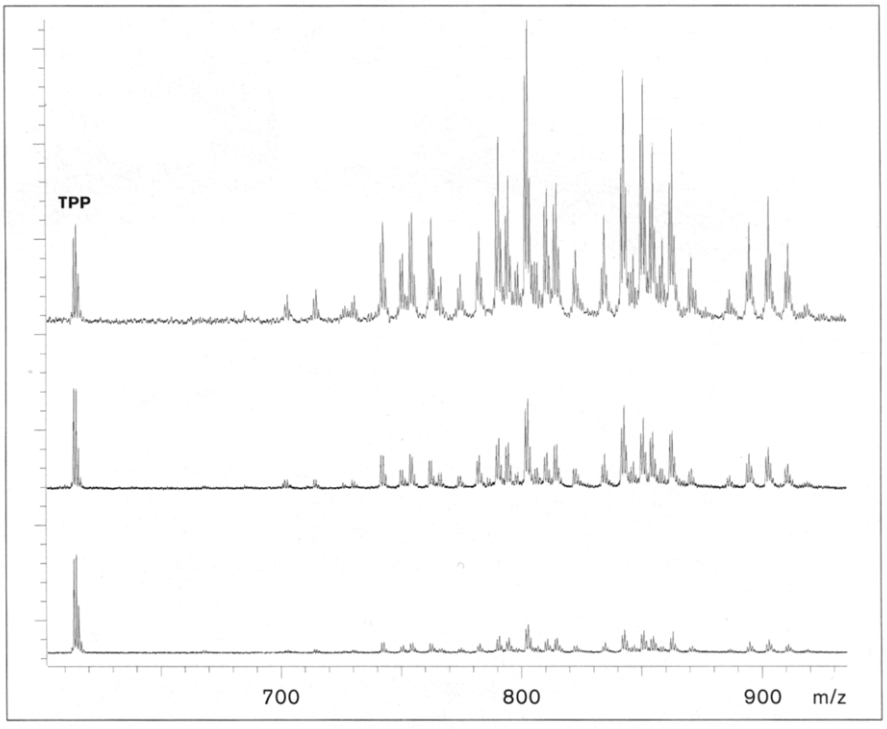


be prepared from four building blocks were scanned in the same meta-library structure space, and a library leading to an overlap-free mass spectrum was identified (Fig. 2, **Library II**). **Library II** contains 35 non-isobaric compounds, 19 of which appear in the form of two or more isomers. MALDI-TOF spectra of **Library II** are shown in Figure 4.

The libraries of porphyrin acids (Fig. 2b) and peptide–DNA hybrids (Fig. 2c) employed in this study are less complex and were chosen without resorting to computational methods.

### Quantitative MALDI-TOF MS

The first step in optimizing MALDI-TOF MS for quantitative analysis of tetraphenylporphyrins, porphyrin acids,

**Figure 5**

Typical calibration curves used for quantifying components contained in **Library II**. The curves were derived from spectra including those shown in Figure 4. The ratios of peak height between analyte and internal standard (TPP) from five individual spectra (mean ± one standard deviation) are plotted versus total porphyrin concentration. Differences in the slope of regression lines are mostly due to different concentrations of compounds, which in turn are a result of the peculiarities of the combinatorial synthesis of highly symmetrical compounds such as tetraphenylporphyrins. See Figure 2a for structural formulae. TF=$CF_3$.

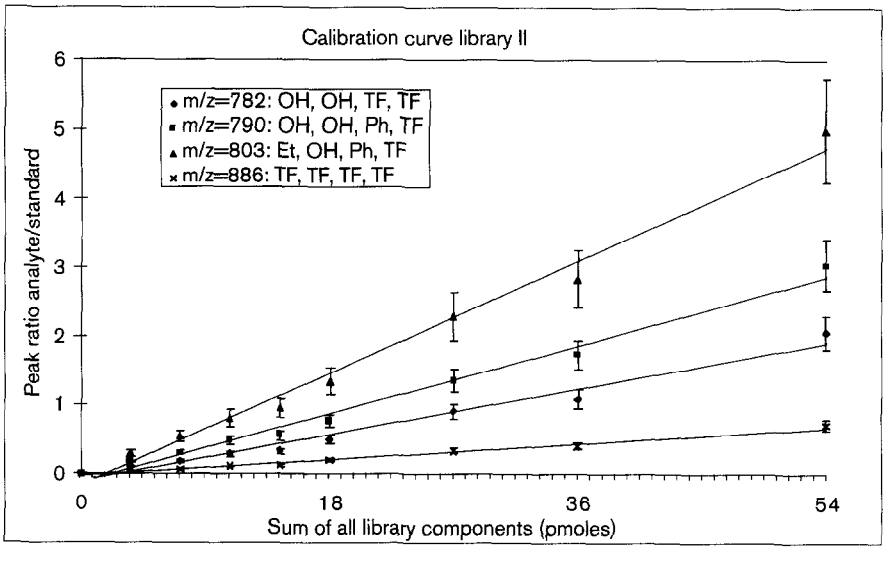

and peptide-DNA hybrids involved screening different matrices. 3,4- and 2,5-dihydroxybenzoic acid, 2-(4-hydroxyphenylazo)benzoic acid, α-cyano-4-hydroxycinnamic acid, 2,4,6,-trihydroxyacetophenone (THAP), and 6-aza-2-thiothymine were tested under a number of different crystallization conditions. Spectra were acquired in all available acquisition modes (negative or positive, linear or reflectron, delayed extraction or continuous extraction) in order to find conditions that led to peak patterns reflecting those calculated by the prediction algorithm of MASP.

Libraries of tetraphenylporphyrins gave best results when laser desorption spectra were acquired without matrix from a thin film of the porphyrins prepared by fast evaporation of a solution in $CH_2Cl_2$:MeOH (4:1). Spectra acquired in reflectron mode gave sufficiently high signal-to-noise ratios and were better resolved than spectra acquired in linear mode, as expected for the extended ion path (1.6 versus 1.2 m in our instrument). The positive ion mode gave sufficient signal-to-noise ratios while the negative mode gave hardly any signal. A comparison of a predicted and an acquired laser desorption spectrum of a tetraphenylporphyrin library containing 120 compounds and 70 non-isobaric compounds is shown in Figure 3. The mixture of the more polar porphyrin acids required the use of a matrix to achieve sufficient signal-to-noise ratios. Interestingly, THAP, a matrix developed for oligonucleotides, gave best results when combined with ammonium tartrate as comatrix and DMSO as an additive. This may be partly due to the net negative charge on both porphyrin acids and nucleic acids. Positive reflectron mode with delayed extraction was the most successful acquisition parameter combination. Even with this matrix, the highly polar heptaacid and octaacid **5** and **6** (Fig. 2b) could not be desorbed with a similar efficiency to **1–4**, and consistently gave smaller mass peaks than predicted. Peptide–DNA hybrids gave the predicted mass spectra with THAP as matrix and ammonium citrate as comatrix in linear, negative-mode, conditions that have previously been used for oligonucleotides [23], demonstrating that the DNA part dominates the desorption properties of the hybrids. Without the ammonium citrate comatrix, the $Na^+$ and $K^+$ adducts were abundant.

**Figure 6**

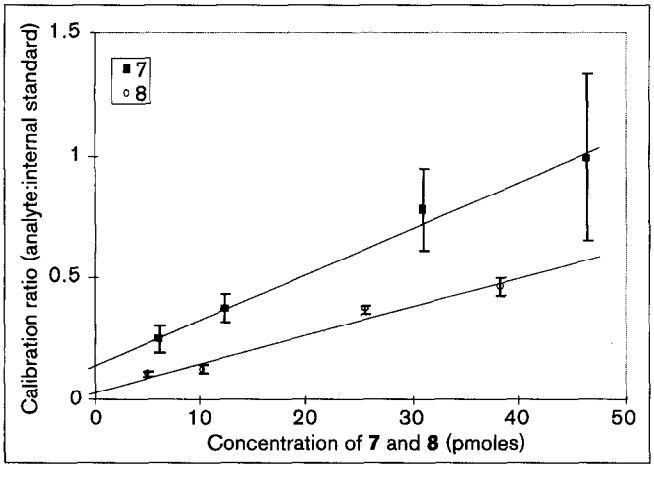


Calibration curves for the quantitation of peptide–DNA hybrids **7** and **8**, using **9** as an internal standard. Peak height ratios (analyte/internal standard, mean ± one standard deviation of six spectra) were plotted against concentrations of **7** and **8**. See the Materials and methods section for experimental details.

The next step in our study was to establish quantitative, reproducible, signal–concentration relationships. Three main strategies were pursued: first, an internal standard was added and peak ratios, rather than absolute peak intensities, were measured; second, the fluence of the laser was increased to *ca.* 50% above the threshold for ion production; and third, several spectra of ≥100 shots each were acquired per data point and the mean ± standard deviations for the analyte/internal standard peak ratios was calculated. The increase in laser irradiance and the accumulation of laser shots for every spectrum was particularly critical for obtaining reproducible peak ratios from the porphyrin acid mixture. Often, peak ratios changed during the acquisition of spectra to reach a stable plateau after *ca.* 50–75 high energy shots. The ion production usually ceased after 100–150 laser shots, indicating that the spot was exhausted. This, and discernible holes in the matrix after the acquisition of spectra indicated that full ablation of the matrix–analyte mixture was necessary in this case to achieve reproducibility. The high laser fluence and the increased number of shots per spectrum led to an appreciable loss of resolution. We found that delayed extraction desorption [24] strongly decreased this broadening effect. Furthermore, lowering the extraction voltage (and thus prolonging the flight time of the ions) increased the resolution without decreasing the ion counts dramatically. A lowered extraction voltage was used for the porphyrins. At a digitizer sampling rate of 1 GHz, a spectral window of 1000 mass units and delayed extraction at 10 kV in reflectron mode, a half-height peak width resolution of 2000 was routinely achieved for these less polar porphyrins. This is shown for **Library II** in Figure 3b. Tetraphenylporphyrin (TPP) was used as internal standard. Linear calibration curves over a concentration range of more than one order of magnitude were measured for all 32 detectable porphyrin compounds of this library, shown for selected compounds in Figure 5. The dynamic range was larger than one order of magnitude, however, as the abundance of individual compounds within the library varies by a factor of 24 due to the statistics of the combinatorial synthesis. Linear calibration curves for peptide–DNA hybrids **7** and **8** were obtained when **9** was used as internal standard (Fig. 6). Spectra in delayed extraction, linear detection mode showed a resolution of *ca.* 400 at the necessary high laser fluence at

1.2 m flight path. This was sufficient for selectively detecting **7** and **8**, whose molecular weights differ by only 6 mass units. Depending on the amplifier gain of the detector, saturation effects became evident at quantities of 75 picomoles or higher. Detailed acquisition parameters and instrumental settings used for quantitative MALDI detection of all three classes of analytes are given in the Materials and methods section.

### SMOSE assays

*Liposome incorporation of tetraphenylporphyrins*

Using the quantitative MALDI detection mode, incorporation of the porphyrins of **Library II** in phospholipid membranes was assayed. The procedure for preparing the liposomes has been reported previously [25]. A partitioning between the membrane and aqueous phase occurs during the formation of lamellar phases induced by treating a lipid-porphyrin film with aqueous buffer. The resulting multilamellar liposomes are then subjected to exhaustive sonication to form small, unilamellar vesicles, a treatment that is most likely to help achieve the partitioning equilibrium. Control experiments confirmed that the macroscopic incorporation efficiency of porphyrin libraries was reproducible within 10%. Quantitative MALDI-TOF spectra of samples taken from the liposome and the precipitate fraction were acquired to study the partitioning of the individual porphyrin species. Reflectron MALDI spectra of the liposome fractions were essentially undisturbed by dioleylphosphatidylcholine (DOPC) but the signal-to-noise ratio was lower than that found in spectra of lipid-free samples. Accordingly, the lipid was removed by filtration over silica. Control experiments with **Library II** showed that the silica did not retain any porphyrins and did not bias the library. Liposome incorporation efficiencies were calculated from the peak intensities in the MALDI spectra of liposome and precipitate fractions (Fig. 7). A percentage of each of these non-water-soluble porphyrins was incorporated in the DOPC membranes, and a fraction precipitated from the aqueous buffer. When a 20-fold molar excess of lipid over total porphyrins was employed, more than 60% of every library member was found in the liposomes and less than 40% in the precipitate. A small fraction was lost due to adsorption to the metal tip of the probe sonicator. The structure space of tetraphenylporphyrins combinatorially synthesized from a mixture of four phenyl aldehyde building blocks is difficult to present in two dimensions. We have chosen the representation displayed in Figure 8, where some compounds are represented in more than one bar to enable structure–activity relationships to be read easily. The structure–liposome incorporation relationship map showed linearly additive effects when phenyl substituents were 'exchanged' with hydrocarbon substituents, but non-linear relationships when porphyrins bearing hydrocarbon substituents are compared to those bearing polar groups such as hydroxyl or trifluoromethyl groups. Porphyrins

**Figure 7**

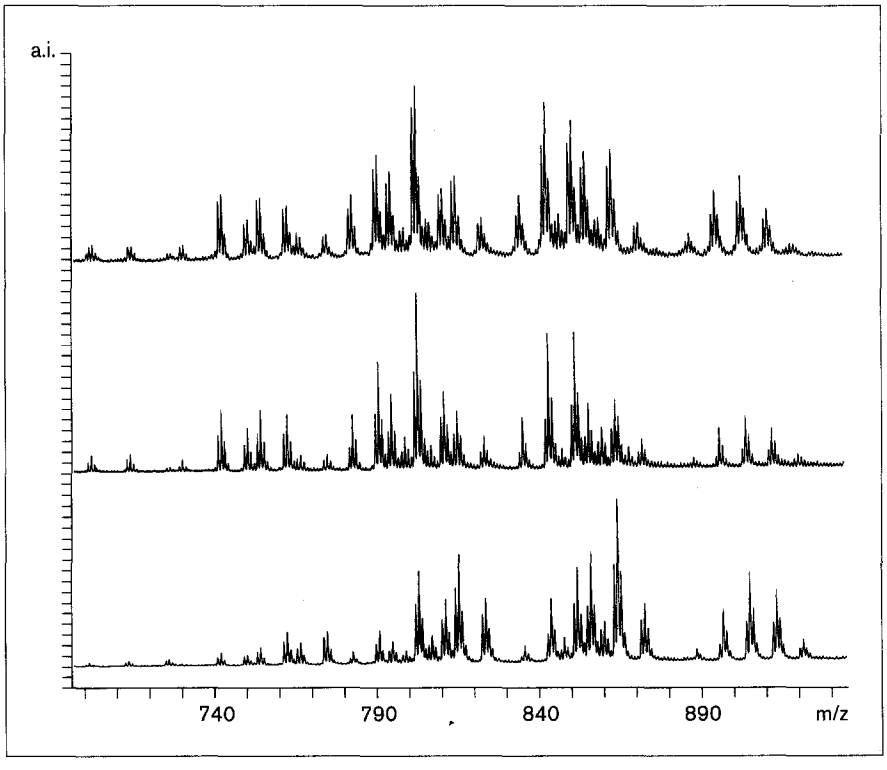


Typical quantitative MALDI-TOF MS of **Library II** undergoing a selection based on liposome incorporation. Top spectrum, prior to the selection assay; middle spectrum, liposome-incorporated fraction; bottom spectrum, non-liposome incorporated fraction (precipitate). Comparison of the spectra shows that peak height enhancements and depletions are complementary in the middle and bottom spectra as expected for a selection based on a partitioning between two phases. Middle and bottom spectra are expanded to show the relative concentrations of compounds. The ratios of absolute concentrations of total porphyrins in liposome and precipitate fraction is 83:17.

bearing the latter type of substituents showed a shallow maximum in the incorporation efficiency when two or three polar substituents and one or two lipophilic substituents were present. Hydroxy-substituents (Figure 8, left panel, rear corner in the bar plot) promoted membrane incorporation particularly strongly. Interestingly, the compounds bearing one hydroxy group had uniformly high incorporation rates, almost independent of the remaining substituents.

*Binding of porphyrin-acids to myoglobin*

Monitoring the porphyrin mixture **1–6** undergoing selection experiments was more challenging than monitoring **Library II** due to the very strong polarity differences between the components of the mixture **1–6**. The ability of the components to bind to the heme pocket of myoglobin was assayed. For this assay, the mixture **1–6** was supplemented with one molar equivalent of hemin, to give a library in which one component was the natural cofactor for the Met-myoglobin form of the holoenzyme. Incubation of this mixture with a myoglobin reconstituted with deuteroporphyrin, a non-natural cofactor for this protein, led to a specific exchange of deuteroporphyrin for hemin. Spectra of the porphyrin library prior to and after the incubation with the deuteroporphyrin-loaded myoglobin are shown in Figure 9. The spectrum acquired after the equilibration with the protein lacks the hemin and shows a distinct peak for deuteroporphyrin. The signal-to-noise ratio in these spectra was poor unless the myoglobin was removed by filtration over a membrane. The hexaacid, heptaacid and octaacid **4–6** were found to be partly depleted after the filtration, which might be due to nonspecific adsorption or aggregation phenomena. Optimized matrix conditions are expected to make the filtration step unnecessary. As expected from the literature [26], diacid **1** also bound to myoglobin when the mixture of **1–6** and hemin was incubated with solutions containing some free apomyoglobin and the deuteroporphyrin-bearing non-natural holoprotein (data not shown).

*Nuclease survival of peptide–DNA hybrids*

The third type of selection experiment performed involved a degradation reaction where the disappearance of full length peptide–DNA oligomers over time was

**Figure 8**

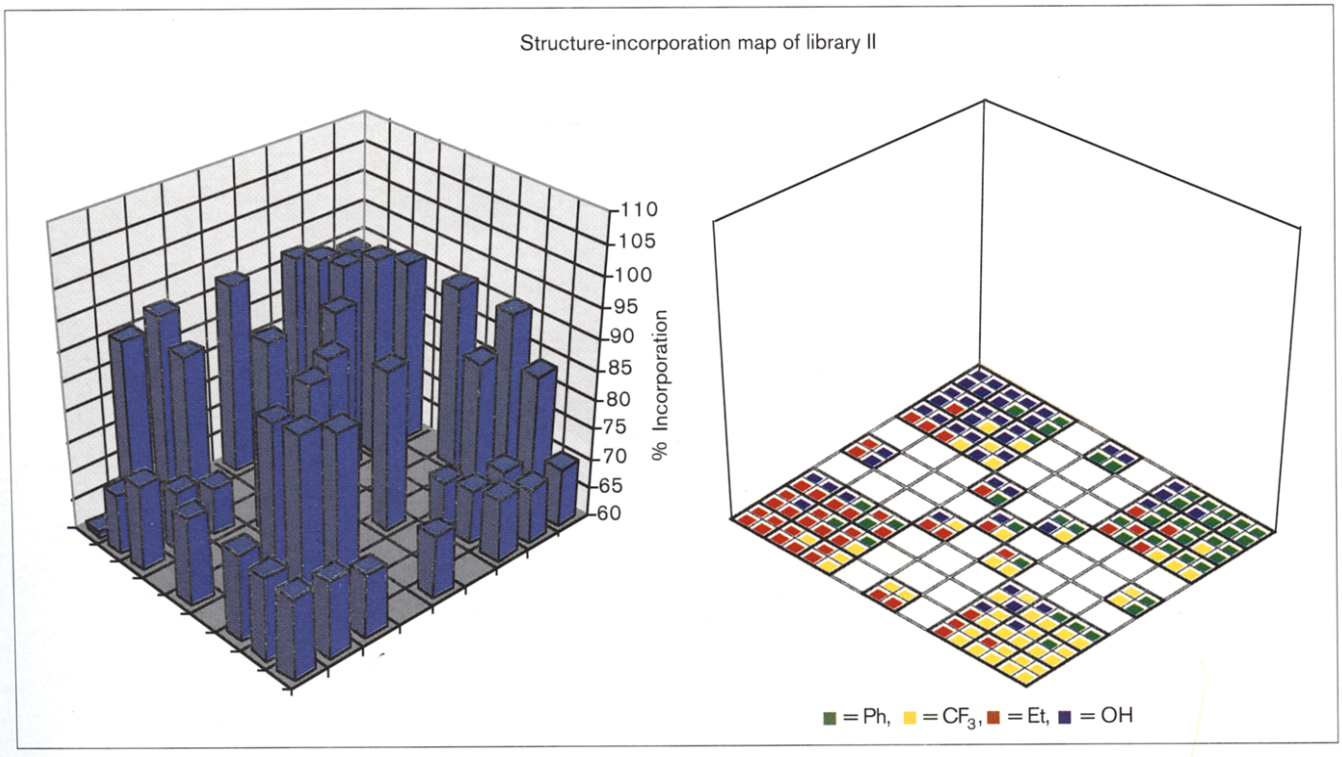


Three-dimensional representation of the structure–activity relationship for liposome incorporation observed for the compounds contained in **Library II**, based on results including the spectra shown in Figure 7. The *z* axis of the bar graph on the left is expanded and covers the range of 60–110% incorporation. It shows the liposome incorporation efficiency of individual compounds. The graph on the right serves as a superimposable legend for the identification of compounds. Every square of four colored dots in the graph on the right hand side corresponds to one blue bar in the graph on the left hand side. Every colored dot in the graph on the right represents one para-substituent of a tetraphenylporphyrin. Isomers are isobaric and cannot be distinguished. Some components appear more than once to improve the recognizability of structure-activity relationships. The incorporation efficiencies represented by the heights of the bars in the left plot are associated with standard deviations of $\leq \pm 4\%$ (average $\pm 2\%$).

**Figure 9**

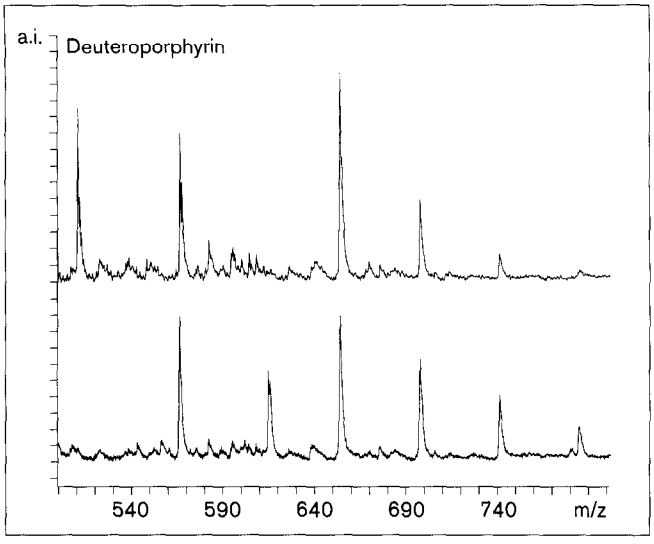


MALDI-TOF-analyzed selection experiment based on the binding affinity of porphyrins to myoglobin reconstituted with the non-natural cofactor deuteroporphyrin. Bottom spectrum: library consisting of porphyrin acids **1–6** and hemin prior to incubation with the deuteroporphyrin-holoprotein. Top spectrum: solution of the porphyrin mixture after 18 h incubation time (compound **6** not shown). The competition leads to the disappearance of free hemin, the natural cofactor, from the solution and the appearance of replaced deuteroporphyrin. See the Materials and methods section for experimental details.

**Figure 10**

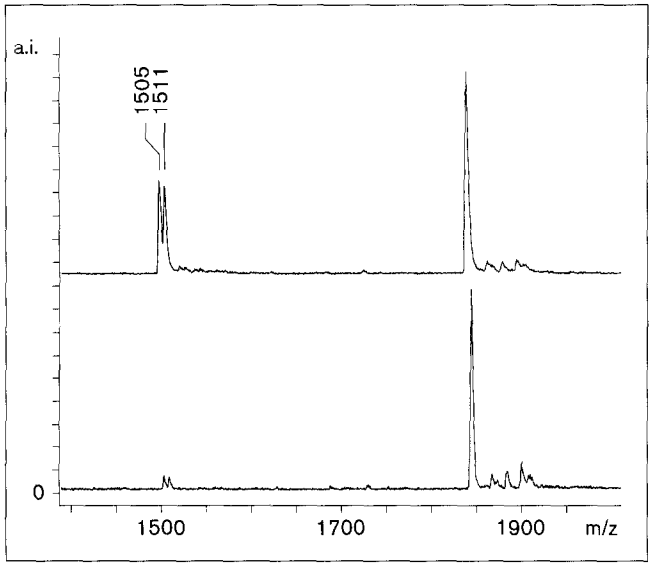


Typical quantitative MALDI-TOF mass spectra of peptide–DNA hybrids **7** and **8** undergoing degradation by phosphodiesterase I. The molecular weight difference between the two analytes is 6 Da. Spectra show an additional peak of **9**, the internal standard added to the matrix preparation. Top spectrum: mixture of **7** and **8** prior to degradation; bottom spectrum: mixture of **7** and **8** after **5** min reaction time.

monitored. This assay mimics the situation in the blood stream where nucleases are known to hydrolyze oligonucleotide-based therapeuticals [27]. We used snake venom phosphodiesterase (EC 3.1.4.1), which hydrolyzes nucleic acids at the 3′ terminus to liberate 5′ nucleotides, and performed the reaction in a 13 mM ammonium acetate buffer. Peptide–DNA hybrids **7** and **8** were degraded simultaneously, and the spectra were acquired with **9** as the internal standard (Fig. 10). Both 5′-modified DNA trimers **7** and **8** were degraded to less than 10% of their initial concentration. Both hybrids contain the same peptide and lose a pyrimidine nucleotide in the first step of the degradation. They are, therefore, expected to react at the same rate and this is what the kinetics of the two reactions show (Fig. 11), demonstrating that this assay is valid for selection experiments. Even small differences in nuclease stability can be monitored with this assay. 'Survivors' may be easily identified in mass spectra of more complex libraries containing nuclease-resistant components.

## Discussion

### SMOSE technique

Several features of the SMOSE methodology make this technique useful for chemical biology, medicinal chemistry, biochemistry, physical organic chemistry, and other related fields. First, this technique promises to be more efficient than traditional assaying of single compounds. Our results indicate that between 2 and 32, and possibly up to *ca.* 100 compounds may be tested in one experiment. This number may be sufficient for a search in a large structure space as small libraries can be designed [28] and can evolve to produce highly active inhibitors when the *in vitro* evolution is guided by a genetic algorithm [29]. Second, SMOSE selection experiments can be performed for a large variety of compounds without the need for labeling or sequencing. Any process associated with a change in concentration or mass may be monitored, including most chemical reactions. In particular, low specificity equilibria in solution, such as membrane partitioning, can be measured where conventional selection experiments would most probably not be successful; the 'activity' differences between library components are small and difficult to detect or amplify with sufficient accuracy. Third, the method requires no more than picomole quantities of library components and provides detailed information on the activity and purity of analytes. Because MALDI-TOF MS is insensitive to most buffer salts, and tolerates impurities and the presence of small quantities of enzymes, time-consuming work-ups or staining steps can be avoided.

SMOSE as an analytical technology has several limitations. It requires libraries to be designed to avoid uninterpretable mass spectra with severe peak overlap. Because mass spectra are predictable and diversity in structure is usually associated with diversity in molecular weight, this limitation does not appear to be very severe. We have designed a

**Figure 11**

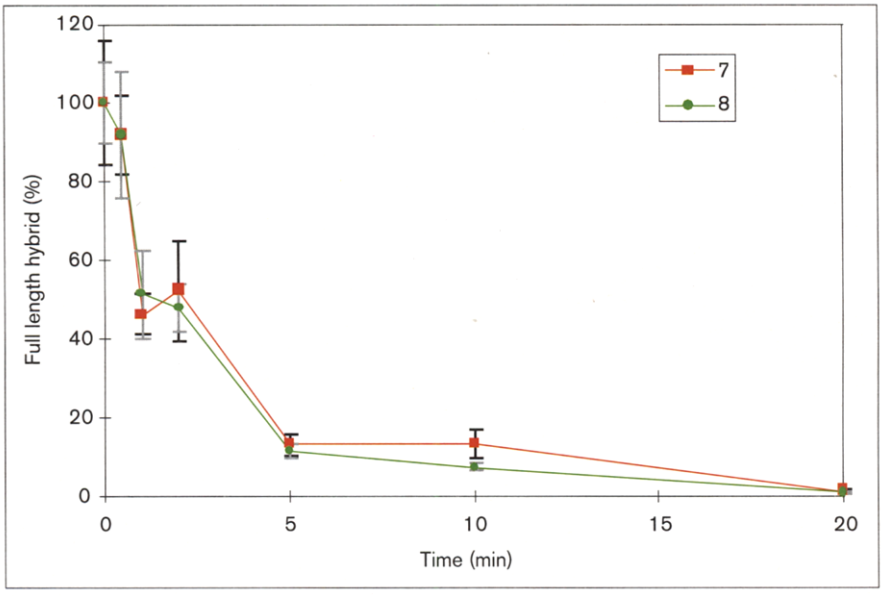


Kinetics of the degradation of peptide–DNA hybrids **7** and **8** by phosphodiesterase I. Analysis by internal-standard-based quantitative MALDI-TOF MS. Based on spectra including those shown in Figure 10.

computer program to assist library design, MASP [22]. The existence of mass spectrometrically indistinguishable isomers can also be limiting when using SMOSE. This problem may be addressed by randomizing only a small number of positions in oligomers. Lead compounds undergoing optimization are often systematically modified at only one position. Finally, SMOSE experiments require access to a MALDI-TOF mass spectrometer and optimization of acquisition parameters. Fortunately, MALDI-TOF spectrometers are commercially available at moderate cost and matrices for a large number of analytes have been reported in the literature. Some effort has to be invested in establishing experimental conditions for quantitative MALDI-TOF-MS, such as the use of DMSO for preventing rapid porphyrin crystallization, which improved the reproducibility of spectra of porphyrin acids **1–6**. From our experience, this time investment quickly pays off as it leads to an extremely versatile technique where structure assignment from spectra is essentially instantaneous.

## Selection experiments

### *Membrane incorporation*

The results of the incorporation assay are relevant to the activity of porphyrins as photosensitizers for photodynamic therapy of tumors. It has been suggested that membranes are among the most sensitive subcellular targets for photodynamic damage [30]. This hypothesis was supported by the reported correlation between lipophilicity and *in vitro* activity of porphyrins and porphyrinoids [31]. From the measurements of the partitioning of other substituted compounds between n-octanol and water by Hansch and coworkers [32], it might be expected that lipophilic substituents contribute a virtually constant increment to the membrane 'solubility' of porphyrins. This seems to be the case for ethyl groups exchanged for phenyl groups (Fig. 8). Other observed structure–membrane incorporation relationships were less linearly predictable based on lipophilicity. Substituents with negative hydrophobicity constants, for example the acetoxy and hydroxy groups, might have been expected to decrease membrane incorporation [33]. This was indeed the case for acetoxy groups, but the more hydrophilic hydroxy substituents markedly increased membrane incorporation (data not shown). We hypothesize that this is due to amphiphilicity, that is the favorable interactions of the hydroxy groups with the polar region of the membranes. The hydrogen bond donor capabilities of the OH functions, their size and their high hydrophilicity might make them more efficient in conveying amphiphilicity than the ester groups. The assumption of amphiphilicity is supported by the observation that one or two hydroxyl groups are sufficient for promoting membrane incorporation (Fig. 8). The results of our selection experiments suggest that hydroxyphenylporphyrins should be highly active photosensitizers for photodynamic inactivation of tumors. This is in excellent agreement with experimental findings. Tetrahydroxyphenyl- porphyrins and their chlorin derivatives have independently been shown to be very efficient photosensitizers of cultivated tumor cells and have been selected for clinical trials [34].

We have been able to measure the concentration of a library of 32 combinatorially synthesized tetraphenylporphyrins on the level of the individual compounds. Membrane-soluble tetraphenylporphyrins other than the compounds rich in hydroxy groups were observed in the structure–membrane incorporation map obtained for this

library (Fig. 8). These compounds are currently being subjected to additional selection experiments and their ability to photoinactivate cultivated tumor cells is under investigation. Although our SMOSE results do not allow isomers of para-substituted tetraphenylporphyrins to be assigned we are not aware of any other spectroscopic technique other than X-ray crystallography that would reveal the isomeric identity of such porphyrins.

*Exchange of myoglobin cofactors*

We chose the competitive reconstitution of myoglobin [26] with a small library of hemin and porphyrin derivatives, containing an increasing number of propionate sidechains, as a selection reaction involving specific recognition of the ligand. The porphyrin library was a commercially available mixture of porphyrin acids. The myoglobin reconstitution reaction has been studied in great detail for sperm whale myoglobin. It was known that the reconstitution from apomyoglobin with an unoccupied binding pocket is unspecific. Equal incorporation rates for differently substituted hemins and two complexation states, different by rotation about the α–γ meso axis are observed [26]. We used myoglobin from horse skeletal muscle as the sperm whale (*Physeter catodon*) is an endangered species. Our competitive reconstitution reaction similar to that previously reported by La Mar and

**Figure 12**

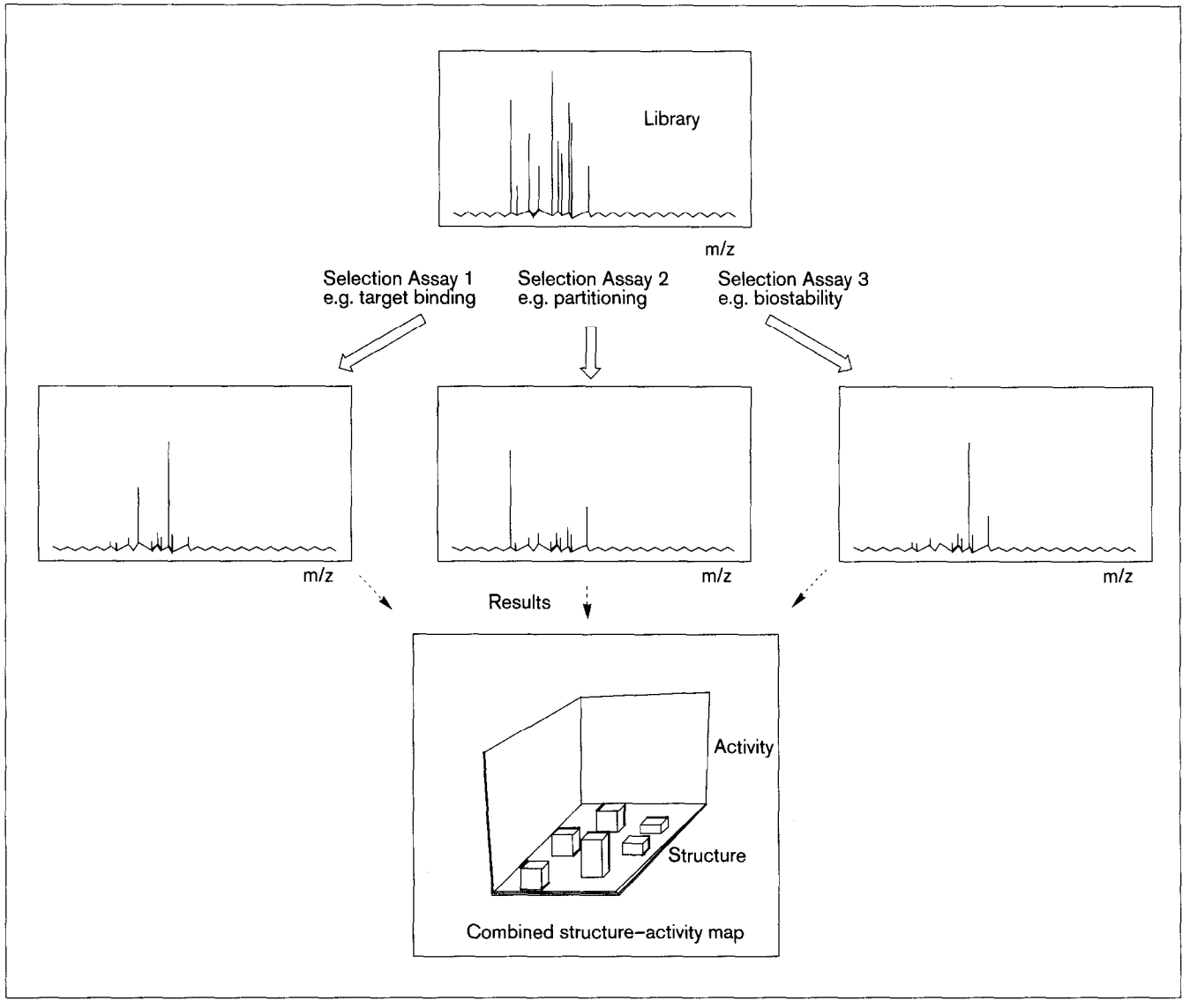


Schematic representation of the proposed 'multidimensional SMOSEs'. A library whose components can be monitored simultaneously by quantitative MALDI-TOF MS is subjected to several selection assays in parallel. The structure–activity information obtained in the individual assays is combined to produce a single structure–activity map where compounds can be picked that show a combination of favorable properties.

collaborators [26], which involves replacing of the non-natural cofactor deuterohemin by hemin or the competitors in the library (Fig. 9). The denaturation and reconstitution of skeletal muscle myoglobin with hemin has previously been monitored by electrospray mass spectrometry in an experiment where the protein peaks were analyzed exclusively [35]. Sperm whale myoglobin, whose binding pocket varies from that of equine myoglobin by the substitution of $Lys^{45}CD3$ (horse) with $Arg^{45}CD3$ (whale), is known to accommodate a third propionic acid substituent in the binding pocket without difficulty [36], but not two additional propionate sidechains [36]. It was also known that iron-free protoporphyrin forms complexes with sperm whale apomyoglobin [37]. When partially deuteroporphyrin-loaded myoglobin was employed in the experiment, both the non-metallated diethyl diacid **1** and hemin were depleted from the library after incubation with the protein, in agreement with these literature reports. Under more competitive conditions, the high specificity expected [26,38] for hemin was observed, demonstrating the validity of our SMOSE assay. Such protein-specific selection experiments select binders, such as inhibitors in solution, without a need for any labeling, tagging or immobilization of the library components.

*Nuclease stability*

Oligonucleotide-based therapeuticals such as antisense inhibitors of gene expression [27] or DNA strands for gene therapy [39] are among the most promising class of compounds for implementing 'molecular medicine.' A major obstacle to their successful use, however, is the rapid degradation of unmodified DNA and RNA by nucleases when they are injected into the blood stream. Nuclease stability is therefore routinely measured as part of the evaluation of modified nucleic acids designed to act as antisense agents. Our results for peptide–DNA hybrids demonstrate how the search for biostable nucleic acid based agents may be performed by combinatorial synthesis and *in vitro* selection. A study with larger libraries involving DNA-binding peptides conjugated to DNA, currently under way in these laboratories, will show whether a protective effect of the peptide can be selected for.

**Multidimensional selections: a hypothesis**

Compounds that show high affinity for a pharmaceutical target, for example a protein, have to fulfill additional criteria to become successful drugs. The ability to overcome membrane barriers and sufficient biostability are two such criteria. These are particularly challenging for the more complex therapeutic agents proposed for molecular medicine [40]. Our studies on liposome incorporation and nuclease stability demonstrate that selections for such 'bioavailability properties' can be performed. 'Activity' differences found in our assays are smaller than those typically found in assays based on a specific binding event, making a quantitative analysis of the results mandatory.

In an expansion of our results shown here, we suggest that a given library may be subjected to several monitored selection experiments in parallel: one for target binding and two or more for properties relevant to bioavailability or target selectivity (Fig. 12). An individual compound in a library may be rated according to its performance in all selection assays, leading to a value in a combined- or meta-structure–activity map. It is in these structure–activity maps that compounds constituting the ideal compromise of several criteria necessary for becoming a successful drug may be identified. We suggest that such experiments are referred to as 'multidimensional selection experiments'.

## Significance

Quantitative MALDI-TOF mass spectrometry of limited-size libraries can be used to monitor *in vitro* selection experiments. In principle, any process leading to a change in concentration or in mass can be detected. This includes, for example, affinity-based selections, most chemical reactions, and partitioning between phases. In the work reported here, libraries of 32 tetraphenylporphyrins, six porphyrin acids, and two peptide–DNA hybrids were simultaneously analyzed on the level of their individual non-isobaric components. These libraries were employed in MALDI-TOF-analyzed multi-analyte assays selecting for liposome incorporation efficiency, protein binding and nuclease stability. In the case of tetraphenylporphyrins, it was found that hydroxy rather than lipophilic substituents promote incorporation in liposome membranes. Hydroxyphenylporphyrins are known to be highly efficient sensitizers for photodynamic therapy of tumors. Other drugs could be optimized using similar assays because the number of analogs initially prepared after identifying a lead compound is often similar to the size of the libraries employed here. This would also be the case where the lead compound was identified by screening a combinatorial library [41]. Furthermore, a search in a larger structure space may be performed with evolving libraries guided by a genetic algorithm [29].

So far, it is mostly medicinal and bioorganic chemists who have benefited from the efficiency of combinatorial synthesis and *in vitro* selection. It seems, however, as if this approach could be useful in many other fields of chemistry, physics and biology. For many assays, experimental details would have to be adapted and mass spectrometry parameters would have to be optimized. The prospect of being able to measure both structure–activity and structure–reactivity relationships, such as a linear free enthalpy relationship, in a single experiment should justify this effort.

## Materials and methods

### *General*

1,2-Dioleoyl-sn-glycero-3-phosphocholine (DOPC), dimethylsulfoxide (DMSO, 99.5%), and diammonium tartrate (99%) were from Fluka. Phosphodiesterase I (type VII, 0.2 unit $mg^{-1}$) was from Sigma. 2,4,6-Trihydroxyactephenone monohydrate (THAP), 5,10,15,20-tetraphenylporphine (TPP, 99%), and ammonium citrate (dibasic, 98%) were from Aldrich. Chloroform (Omnisolv™), and $CH_2Cl_2$ (99.5%) were from EM Science. The latter was distilled over anhydrous calcium chloride prior to use. Methanol was from Baker (HPLC grade). Silicone oil was from Fisher Scientific (heat bath quality). Phosphate-buffered saline solution (PBS) was made up from NaCl (2 g, 34 mmol), $K_2HPO_4 \cdot 3H_2O$ (0.4 g, 1.75 mmol), $KH_2PO_4$ (0.068 g, 0.5 mmol), KCl (0.05 g, 0.75 mmol), and deionized water (ad 250 ml). Silica gel was from Merck (grade 9385, 230–400 mesh, 60 Å). Porphyrin acids **1–6**, deuteroporphyrin, and hemin were from Porphyrin Products, Logan, Utah and were used as received. **Libraries I** and **II** were prepared by Rothemund-type cyclization reactions involving pyrrole and a set of differently para-substituted benzaldehydes. The syntheses of these libraries and those of peptide–DNA hybrids **7–9** will be published separately. MALDI-TOF spectra were acquired on a Bruker BIFLEX™ spectrometer equipped with a 1 GHz digitizer and a delayed extraction unit operated at 150 ns delay time. Fluences of the $N_2$ laser (337 nm) are reported according to the manufacturers specifications and were not measured independently. A microchannel plate detector was used in linear mode and a photomultiplier detector in reflectron mode. The ion flight path was 1.2 m in linear mode and 1.6 m in reflectron mode. Spectra were acquired at pressures $<1 \times 10^{-6}$ mbar in the drift tube.

### *Quantitative MALDI-TOF MS*

Tetraphenylporphyrins — a solution of the porphyrin library in $CH_2Cl_2$:MeOH (4:1 v/v, 1 ml, *ca.* 100 pmol total, *ca.* 1–20 pmol per single compound) was applied to a MALDI target area of *ca.* 5 $mm^2$ to give a shiny, homogeneous porphyrin film. Best results were achieved when using a microsyringe whose needle touched the target surface during release of the solution. The solution was dried instantaneously with a hairdryer to suppress crystallization. Spectra were acquired in delayed extraction, positive reflectron mode at a resolution of ≥2000. The acceleration voltage was 10 kV with a reflectron voltage of 10.25 kV and a delayed extraction voltage of 7.15 kV. The voltage of the post-source ion-lens was set to +5.9 kV. For each spectrum, laser shots were accumulated until at least 1500 ion counts were obtained for the most intense peak. This typically required between 80 and 500 shots of *ca.* 70–120 μJ/shot at a preamplifier voltage of 2 mV, a detector voltage of 1.7 kV, and the absence of deflection of low mass peaks. These conditions did not lead to 'flat-topping' of peaks (saturation effects). Laser fluences at the threshold for ion production (*ca.* 50–60 μJ/shot) gave poorly reproducible results and biased spectra of libraries toward less polar components. Porphyrin spectra acquired under matrix-free conditions showed a combination of $M^{\cdot+}$ and $[M+H]^+$ ions. For calibration curves, a solution of tetraphenylporphyrin (TPP) in $CH_2Cl_2$ (32.6 μM, 2 μl, 65.2 pmol) was added to aliquots (20–300 μl) of a solution of a library in $CH_2Cl_2$:MeOH (4:1 v/v, 56 μM total porphyrin). The volume was adjusted to 302 μl and five spectra per concentration were measured as detailed above. The peak of the most abundant isotope of TPP (internal standard, m/z 614) and analytes were measured using Bruker XTOF software. The mean ± one standard deviation of the height ratios of analyte versus TPP of five spectra were calculated. Since the concentration of individual library components differed by a factor of 24, calibration curves (Fig. 5) reflect linearity over more than two orders of magnitude. It was critical to hold the laser attenuation constant during quantitative detection experiments. Slightly defocusing the laser improved reproducibility, probably because a larger target area with an increased probability of being representative for the analyte mixture was ablated.

Porphyrin acids — a solution of **1–6** and hemin (75 pmol each) in deionized water:DMSO:ammonium hydroxide (160:40:1, 1.5 μl) was mixed with aqueous diammonium tartrate (0.1 M, 3 μl) and an ethanolic solution of THAP (0.3 M, 10 μl). After thorough mixing, 1 μl of the solution was applied to the MALDI target. The volatile solvents were allowed to evaporate at room temperature and the DMSO was evaporated *in vacuo* in the gate chamber of the MALDI-TOF spectrometer. Six spectra per data point were acquired in positive, delayed extraction, reflectron mode using the same instrumental settings as those used for tetraphenylporphyrins (*vide supra*), except that the laser attenuation was set to produce 145–150 μJ shots. Porphyrin tetraacid **4** was used as internal standard. Peak heights for **1–3**, **5**, and hemin were reproducible within 7–25% standard deviation from the mean. Considerably improved spectral resolution could be achieved by lowering the laser fluence at the expense of markedly decreased peak intensities for **5** and **6**.

Peptide–DNA hybrids — for calibration curves, aliquots of stock solutions of **7**, (6.2 μM), **8** (5.1 μM), and **9** (7.5 μM) in deionized water were mixed at ratios of 1:1:10, 1:1:5, 1:1:2, and 3:3:4 such that the volume of the solution of **9** was constant at 5 μl. Samples were dried by lyophilization and diammonium hydrogen citrate (0.6 μl, 0.1 M) was added. After vortexing and centrifugation, a solution of THAP (1.8 μl, 0.3 M in ethanol) was added followed by vortexing and centrifugation. MALDI targets were coated with silicone oil and excess oil was removed by briefly wiping with towels soaked in $CH_2Cl_2$ and acetone. An aliquot of the matrix-comatrix-analyte mixture (1 μl) was applied to the plate and allowed to dry at room temperature. Spectra of 100 laser shots (60–70 μJ) were accumulated at 2 Hz laser frequency and 5 mV preamplifier voltage, in delayed extraction linear, negative mode at an extraction voltage of 20 kV (18.59 kV delayed extraction voltage, −7.0 kV ion lens voltage). Spectra with ion count ≤1000 for internal standard **9** were deleted. Six spectra were acquired per concentration and peak height ratios were calculated between analytes and **9**. The mean of these ratios ± one standard deviation was used for quantitation (Fig. 6). When instrumental parameters influencing the ion yield, such as the positioning of the laser beam or the voltage on the ion lens, were varied the slope of the calibration curves changed but linear calibration curves were obtained in every case. Control experiments demonstrated that peak ratios were constant within the experimental error when analyte samples containing up to 100 mM ammonium acetate were used.

### *Selection experiments*

Liposome incorporation — a solution of DOPC in $CHCl_3$ (585 μl, 20 mg $ml^{-1}$ 11.7 mg, 15 μM) was mixed with a solution of **Library II** in $CHCl_3$/MeOH (9:1, v/v, 5 ml, 750 nmol) in a 25 ml round bottom flask. Solvents were evaporated to dryness *in vacuo* (aspirator) by rotary evaporation (200 rpm) with the bottom of the flask 0.5 cm above the surface of a water bath at 55°C. A clear, homogeneously colored film was formed, which was dried *in vacuo* for an additional 30 min, leading to small bubbles and 'cracks' in the film. The lipid film was hydrated with PBS (1.5 ml, aliquots of 0.8 ml, 0.4 ml, and 0.3 ml) under argon by swirling glass beads (650 mg, diameter 2–3 mm) in the flask. The turbid suspension was sonicated (Fisher Sonic Dismembranator Model 300, 2 cm tip, relative output 0.55) in a 10 ml plastic beaker (2.3 cm diameter) under argon and cooling in a beaker of water (1 l) at ambient temperature. Four sonication intervals of 5 min each with 30 s waiting periods were applied, leading to a clear, but opaque liposome 'solution'. After 24 h annealing at room temperature in the dark, the sample was centrifuged for 15 min at 2000 g, producing a dark precipitate. The supernatant containing the liposomes was carefully aspired, 0.25 ml were lyophilized, and the residue dissolved in 50 ml $CH_2Cl_2$. The precipitate was dried *in vacuo* and dissolved in $CH_2Cl_2$ (25 ml). The liposome incorporation efficiency (the amount of porphyrins in the liposomes divided by the total amount in liposomes and precipitate) was determined by UV spectroscopy using $\varepsilon_{420}$ 500 000 $M^{-1} cm^{-1}$. Both solutions were dried *in vacuo* and the residues redissolved in $CH_2Cl_2$:MeOH ( 4:1, 0.2 ml). The solution derived from the liposome phase was filtered through a plug of silica in a micro column (4.5 mm diameter, 6 cm column length; $CH_2Cl_2$:MeOH, 4:1 v/v). All fractions

showing fluorescence at $\lambda_{exc}$ 366 nm were combined, evaporated and redissolved in $CH_2Cl_2$:MeOH (4:1, 0.2 ml). 5–7 mass spectra each of the solutions of precipitate and the liposomes respectively were acquired as described above, and analyzed in terms of peak height ratios. The molar ratio of the library components was determined by dividing the peak height of individual peaks through the sum of peak heights of all library members. Control experiments showed that results were similar when peak integration instead of peak height measurements were used for quantitation but standard deviations were higher for the integration mode. Peak height-based quantitation gave relative standard errors between 0.6% and 15% (average 5%).

Exchange of myoglobin cofactors — deuteroporphyrin (200 nmol) was dissolved in a mixture of water and DMSO (4:1, 1 ml, plus 5 µl of concentrated aqueous ammonia to facilitate dissolution). The solution was added dropwise with stirring to a mixture of ammonium acetate solution (100 µl, 1.0 M) and aqueous apomyoglobin solution (250 µl, 74 µM, 18.5 nmol). After 5 min stirring, the solution was allowed to stand at room temperature for 48 h. The deuteroporphyrin-loaded holoprotein was isolated from the solution by filtration over a Centricon 3 ultrafiltration membrane (cutoff 3000 Da), and was washed three times with ammonium acetate buffer (50 mM, 3 × 1 ml). The myoglobin was recovered by centrifugation of the inverted membrane, and was diluted with ammonium acetate buffer (100 mM) to a total volume of 500 µl. A solution of **1–6** and hemin (10 nmol each, 70 nmol total porphyrin) in DMSO:water (4:1, 1 ml, plus 5 µl of concentrated aqueous ammonia to facilitate dissolution) was added, and the mixture was allowed to stand at room temperature for 18 h. The protein was removed by filtration as described above and the filtrate was freeze-dried *in vacuo*. The residue from the filtrate was dissolved in water:DMSO (4:1, 200 µl) and 1.5 µl of the solution were mixed with ammonium tartrate buffer (3 µl, 0.1 M) and a THAP solution in ethanol (10 µl, 0.3 M). MALDI-TOF spectra were acquired as described above.

Nuclease degradation — a solution of phosphodiesterase I ($6.25 \times 10^{-5}$ units per µl, 1 µl) in ammonium acetate buffer (218 mM) was added to a solution of **7** (121 pmoles) and **8** (100 pmoles) in deionized water (26 µl). After quick and thorough mixing, the solution was transferred to a water bath at 37°C. Aliquots (1 µl) were removed after selected periods of time (30 s–20 min) and quickly transferred into a mixture of a solution of **9** (22.6 pmoles) in diammonium hydrogen citrate (0.1 M, 1 µl) and THAP (0.3 M in ethanol, 3 µl) at 0°C followed by immediate thorough mixing. Five spectra per time point were acquired as described above.

### *Supplementary material*

A selected two-dimensional plot of the structure–activity relationship shown in Figure 8 is available with this paper on the internet.

## Acknowledgements

The authors are grateful to Jack E. Greene for performing exploratory experiments on the quantitative MALDI-TOF MS of peptide–DNA hybrids, to David Sarracino for helpful discussions and to Tufts University for support. K.B. was supported by a postdoctoral fellowship from the Stiftung Stipendien-Fonds des Verbandes der Chemischen Industrie, FRG, under the Post Doc-Stipendien VAA program.

## References

1. Thompson, L.A. & Ellman, J.A. (1996). Synthesis and applications of small molecule libraries. *Chem. Rev.* **96**, 555–600.
2. Hansch, C. (1993). Quantitative structure–activity relationships and the unnamed science. *Acc. Chem. Res.* **26**, 147–153.
3. Jaffé, H.H. (1953). A reexamination of the Hammet equation. *Chem. Rev.* **53**, 191–261.
4. Smith, R.D., Loo, J.A., Edmonds, C.G., Barinaga, C.J. & Udseth, H.R. (1990). New developments in biochemical mass spectrometry — electrospray ionization. *Anal. Chem.* **62**, 882–899.
5. Karas, M. & Hillenkamp, F. (1988). Laser desorption ionization of proteins with molecular mass exceeding 10 000 Daltons. *Anal. Chem.* **60**, 2299–2301.
6. Burlingame, A.L., Boyd, R.K. & Gaskell, S.J. (1996). Mass spectrometry. *Anal. Chem.* **68**, 599R–651R.
7. Fitzgerald, M.C. & Siuzdak, G. (1996). Biochemical mass spectrometry: worth the weight? *Chemistry & Biology* **3**, 707–715.
8. Rideout, D., Bustamante, A. & Siuzdak, G. (1993). Cationic drug analysis using matrix-assisted laser desorption/ionization mass spectrometry: application to influx kinetics, multidrug resistance, and intracellular chemical change. *Proc. Natl. Acad. Sci. USA* **90**, 10226–10229.
9. Chen, X. *et al.* & Whitesides, G.M. (1995). Using electrospray ionization FTICR mass spectrometry to study competitive binding of inhibitors to carbonic anhydrase. *J. Am. Chem. Soc.* **117**, 8859–8860.
10. Gao, J. *et al.* & Whitesides, G.M. (1996). Screening derivatized peptide libraries for tight binding inhibitors to carbonic anhydrase II by electrospray ionization-mass spectrometry. *J. Med. Chem.* **39**, 1949–1956.
11. Kupke, T., Kempert, C., Jung, G. & Goetz, F. (1995). Oxidative decarboxylation of peptides catalyzed by flavoprotein EpiD. *J. Biol. Chem.* **270**, 11282–11289.
12. Zhao, Y. *et al.* & Chait, B.T. (1996). Mapping protein–protein interactions by affinity-directed mass spectrometry. *Proc. Natl. Acad. Sci. USA* **93**, 4020–4024.
13. Kriwacki, R.W., Wu, J., Siuzdak, G. & Wright, P.E. (1996) Probing protein/protein interactions with mass spectrometry and isotopic labeling: analysis of the p21/Cdk2 complex. *J. Am. Chem. Soc.* **118**, 5320–5321.
14. Cohen, S.L., Ferre-D'Amare, A.R., Burley, S.K. & Chait, B.T. (1995). Probing the solution structure of the DNA-binding protein Max by a combination of proteolysis and mass spectrometry. *Protein Sci.* **4**, 1088–1099.
15. Boutin, J.A. *et al.* & Fauchere, J.-L. (1996). Combinatorial peptide libraries: robotic synthesis and analysis by nuclear magnetic resonance, mass spectrometry, tandem mass spectrometry, and high-performance capillary electrophoresis techniques. *Anal. Biochem.* **234**, 126–141.
16. Bonnet, R. (1995). Photosensitizers of the porphyrin and phthalocyanine series for photodynamic therapy. *Chem. Soc. Rev.* **24**, 19–33.
17. Kessel, D. & Dougherty, J. (1983). Porphyrin photosensitization. Plenum Press, New York.
18. Pass, H.I. (1993). Photodynamic therapy in oncology: mechanisms and clinical use. *J. Natl. Cancer Inst.* **85**, 443–456.
19. Corey, D. (1995). 480 000-fold acceleration of hybridization by chemically modified oligonucleotides. *J. Am. Chem. Soc.* **117**, 9373–9374.
20. Tung, C.-H., Wang, J., Leibowitz, M.J. & Stein, S. (1995). Dual specificity interaction of HIV-1 TAR RNA with Tat peptide-oligonucleotide conjugates. *Bioconjugate Chem.* **6**, 292–295.
21. Arar, K., Aubertin, A.-M., Roche, A.-C., Mognsigny, M. & Mayer, R. (1995). Synthesis and antiviral activity of peptide–oligonucleotide conjugates prepared by using Na-(bromoacetyl)peptides. *Bioconjugate Chem.* **6**, 573–577.
22. Steinbeck, C., Berlin, K. & Richert, C. (1997). MASP – a program predicting mass spectra of combinatorial libraries. *J. Chem. Inf. Comput. Sci.*, in press.
23. Pieles U., Zürcher W., Schär M. & Moser H.E. (1993). Matrix-assisted laser desorption ionization time-of-flight mass spectrometry: a powerful tool for the mass and sequence analysis of natural and modified oligonucleotides. *Nucleic Acids Res.* **21**, 3191–3196.
24. Vestal, M.L., Juhasz, P. & Martin, S.A. (1995). Delayed extraction matrix-assisted laser desorption ionization time-of-flight mass spectrometry. *Rapid Comm. Mass Spectrom.* **8**, 317–322.
25. Richert, C. (1993). A longtime stable liposome formulation for porphyrinoid photosensitizers. *J. Photochem. Photobiol. B. Biol.* **19**, 67–69.
26. La Mar, G.N., Toi, H. & Krishnamoorthi, R. (1984). Proton NMR investigation of the rate and mechanism of heme rotation in sperm whale myoglobin: evidence for intramolecular reorientation about a heme twofold axis. *J. Am. Chem. Soc.* **106**, 6395–6401.
27. Uhlmann, E. & Peyman, A. (1990). Antisense oligonucleotides: a new therapeutic principle. *Chem. Rev.* **90**, 544–584.
28. Sheridan, R.P. & Kearsley, S.K. (1995). Using a genetic algorithm to suggest combinatorial libraries. *J. Chem. Inf. Comput. Sci.* **35**, 310–320.
29 Weber, L., Wallbaum, S., Broger, C. & Gubernator, K. (1995). Optimization of the biological activity of combinatorial compound libraries by a genetic algorithm. *Angew. Chem. Int. Ed. Engl.* **34**, 2280–2282; *Angew. Chem.* **107**, 2452–2454.

30. Moan, J. (1986). Porphyrin-sensitized photodynamic inactivation of cells: a review. *Las. Med. Sci.* **1**, 5–11.
31. Moan, J., Peng, Q., Evensen, F., Berg, K., Western, A. & Rimington, C. (1987). Photosensitizing efficiencies, tumor and cellular uptake of different photosensitizing drugs relevant to photodynamic therapy of cancer. *Photochem. Photobiol.* **46**, 713–721.
32. Leo, A., Hansch, C. & Elkins, D. (1971). Partition coefficients and their use. *Chem. Rev.* **71**, 525–616.
33. Fersht, A. (1985). Enzyme Structure and Mechanism. (2nd edn). pp. 299–301, W.H. Freeman and Company, New York.
34. Ris, H.-B., *et al.* & Althaus, U. (1991). Photodynamic therapy with chlorins for diffuse malignant mesothelioma: initial clinical results. *Br. J. Cancer* **64**, 1116–1120.
35. Katta, V. & Chait, B.T. (1991). Observation of the heme-globin complex in native myoglobin by electrospray-ionization mass spectrometry. *J. Am. Chem. Soc.* **1991**, 8534–8535.
36. Hauksson, J.B., La Mar, G.N., Pandey, R.K., Rezzano, I.N. & Smith, K.M. (1990). NMR study of heme pocket polarity/hydrophobicity of myoglobin using polypropionate-substituted hemins. *J. Am. Chem. Soc.* **112**, 8315–8323.
37. La Mar, G.N., Pande, U., Hauksson, J.B., Pandey, R. & Smith, K.M. (1989). Proton nuclear magnetic resonance investigation of the mechanism of the reconstitution of myoglobin that leads to metastable heme orientational disorder. *J. Am. Chem. Soc.* **111**, 485–491.
38. Yee, S. & Peyton, D.H. (1991) Proton NMR investigation of the reconstitution of equine myoglobin with hemin dicyanide. Evidence for late formation of the proximal His93F8–iron bond. *FEBS Lett.* **290**, 119–122.
39. Morgan, R.A. & Anderson, W.F. (1993). Human gene therapy. *Ann. Rev. Biochem.* **62**, 191–217.
40. Jain, R.K. (1996). Delivery of molecular medicine to solid tumors. *Science* **271**, 1079–1080.
41. Stevens, S.Y., Bunin, B.A., Plunkett, M.J., Swanson, P.C., Ellman, J.A. & Glick, G.D. (1996). Non-nucleic acid inhibitors of protein–DNA interactions identified through combinatorial chemistry. *J. Am. Chem. Soc.* **118**, 10650–10651.